Journal of Materials Science Research;Vol. 2, No. 1; 2013
ISSN 1927-0585 E-ISSN 1927-0593
Published by Canadian Center of Science and Education

Wavelet Denoising in Electrical Resistance Based Damage Detection of Carbon Fiber Composite Materials

Jie Wen[1], Fred K. Choy[2] & Zhenhai Xia[3]

[1] Stevenson & Associates, 6611 Rockside Road, Suite 110, Independence, OH, USA

[2] Department of Mechanical Engineering, University of Akron, 302 Buchtel Commons Akron, OH, USA

[3] Department of Materials Science and Engineering, Department of Chemistry, University of North Texas, Denton, Texas, USA

Correspondence: Fred K. Choy, Department of Mechanical Engineering, University of Akron, 302 Buchtel Commons Akron, OH 44325, USA. E-mail: fchoy@uakron.edu

Received: October 15, 2012 Accepted: November 2, 2012 Online Published: December 5, 2012

doi:10.5539/jmsr.v2n1p82 URL: http://dx.doi.org/10.5539/jmsr.v2n1p82

Abstract

As carbon fiber reinforced polymer composites (CFRPs) are multifunctional materials in which the damage is coupled with the change in material electrical resistance, the use of electrical conductivity monitoring can provide real-time information concerning the damage state through examining the change in resistance/electric potential. It has been shown that, in some recent work, resistance measurement allows the monitoring of the in-situ evolution of various internal damage nucleation and growth phenomena such as fiber fractures, interply matrix cracks and interply delamination. However, one of the common difficulties in measuring the small changes of electrical signals due to failures in the CFRPs is the contamination of extraneous noises during the detection process.

In this paper, signal analysis procedures are applied to minimize or eliminate the contaminated noise during the damage detection process, as to maximize the accuracy of the damage detection process. In addition to the traditional time signal averaging technique, the Fast Fourier Transform (FFT) is applied to filter at the narrow band near the input frequency as to eliminate the unwanted noises. However, based on laboratory experiments, the authors have found that the frequency filtering techniques will retain significant inaccuracy when extraneous noises are in the neighborhood of the input frequency, and, in some cases, accurate measurement of the electrical signals can be susceptable when noise components are significantly higher than the original input signal. To overcome this drawback, the use of a joint time-frequency technique with wavelet transforms has been introduced. As a joint time-frequency signal analysis tool, the wavelet transforms offer simultaneous interpretation of the signal in both time and frequency domains which results in signal filtering effects in both time and frequency domains. Experimental results by the authors have shown significant improvement in accuracy when using the wavelets than those of the FFT and the time averaging techniques. This paper demonstrates the wavelet transform applications in electrical signal noise reduction of CFRPs as well as the use of both continuous wavelet (CWT) and discrete wavelet (DWT) transforms. It has been found that when noise is small, the DWT is more appropriate as the original signal can be reconstructed to offer better comparative information. The use of CWT will provide better results when random noises are significantly higher. Although the use of CWT does not have the ability revert back to the original signal, the comparison of the CWT coefficients can offer more valuable information concerning the damage occurrences while the repeated applications of DWT will result in accumulated errors such that the original shapes of the wavelet cannot be correctly reconstructed.

Keywords: CFRPs, wavelet denoising, damage detection

1. Introduction

Carbon fiber reinforced polymer composites (CFRPs) are manufactured by mixing carbon fibers and plastic resin under certain prescribed conditions for a variety of applications. These materials are distinguished by their high strength and rigidity, high resistances to impact and corrosion, low density, excellent damping properties, and modifiable thermal expansion to complement complex characteristics profile. Based on their excellent mechanical properties, CFRP materials have been widely used for critical components and structures, such as aircraft fuselage and wing structures, helicopter rotors, wind turbine blades, road and marine vehicle body structures, and large civil infrastructures. With the remarkable reduction in weight and extensive increase in strength, the use of CFRPs can provide significant improvements in the efficiency and durability of vehicle components and structural facilities than those using traditional metallic materials.

Under complex environments and loading states, damage of CFRPs in the form of penetration, delamination and/or transverse cracking may occur in these materials during service. Without adequate precautions and health managements, these damages can sometimes lead to catastrophic loss. As an example, the new Boeing 787 structural composition contains over 50% of CFRPs in the fuselage and wing structures. As a result, the consequence from a bird strike can result in an extensive threat for the integrity of the aircraft when a hole shaped damage is initiated within the composite structure. As to ensure the safety and reliability of CFRPs during their lifetime without disassembling the structure, non-destructive evaluation (NDE) has become one of the critical issues in the successful application of CFRPs. Currently NDE has been used as a primary tool for structural damage detection/health monitoring and the prediction of the remaining service life of the CFRP components. Some of the structural damage detection procedures have been further applied to provide life extension control or damage mitigation of critical structural components for operational safety and mission accomplishments. At present, there are various NDE methods that can be used for the assessment of the damage state. Most conventional NDE techniques such as ultrasonic C-scan (Kacmarek & Maison, 1994), x-ray (Trappe & Harbich, 2006), thermography (Bai & Wong, 2001) and eddy current (Mook et al., 2001) are not on-line based detection techniques, and they usually require the targeted component to be taken out of service for a prolonged period of time for post-damage inspection and assessment. Other techniques, such as piezoelectric sensor (Wang & Chung, 1998), optical fiber (Takeda et al., 2002), can be used for real-time on-line health monitoring of CFRP structures but they all require the attachment of external sensors or additional inputs in CFRPs.

The development of a self-sensing damage detection procedure in CFRPs is based on the electrical conductive properties of the carbon fibers. As CFRPs are multifunctional materials in which the damages are coupled with the change in material electrical resistances, the use of electrical conductivity monitoring can provide real-time information concerning the damage state through the change in resistance/electric potential. The uniqueness of this resistivity technique lies in its capability of in-situ self-sensing of damage criticality of composite materials without any additional sensors to be embedded within composites. Currently, experimental work has been conducted relying on the direct monitoring of the electrical conductive characteristics of carbon fibers for damage detection in CFRPs. It has been shown that, in some recent work, resistance measurement allows the monitoring of the in-situ evolution of various internal damage nucleation and growth phenomena such as fiber fractures, interply matrix cracks and interply delamination (Wang & Chung, 2001, 2002). Characteristics of changes in electrical resistance of carbon fiber composite damages have been established by a number of experimental studies in the last decade (Wong & Chung, 1998; Schulte & Baron, 1989).

One of the common difficulties in measuring small changes of electrical signals due to failures in the carbon fibers is the contamination of induced noises due to machinery operation or electrical field in the neighboring environment. This inaccuracy of the damage detection due to noise contamination can be significantly amplified during field operation where noisy operating environment is a typical problem. In this paper, signal analysis procedures are applied to minimize or eliminate the contaminated noise during the damage detection process, as to maximize the accuracy of the damage monitoring/detection process. In addition to the traditional time signal averaging technique, the Fast Fourier Transform (FFT) is applied to analyze signals in frequency domain. With the input signal furnished at a constant sine wave form, the output signal can be filtered at the narrow band near the input frequency to eliminate the unwanted noises. Using this frequency filtering technique, a significant improvement in accuracy can be achieved by eliminating the extraneous noises created at other frequencies in the acquired signal. However, based on numerical experiments, the authors have found that the frequency filtering techniques have two shortcomings; namely, (i) the frequency filtering process will retain data inaccuracy when extraneous noises are near the neighborhood of the input frequency, and (ii) the frequency filtering process is incapable to provide an accurate measurement of the magnitudes of the electrical signals when noise components are significantly higher than the original input signal. To overcome this drawback, the use of a joint time-frequency technique with wavelet transforms has been introduced (Walker, 2008). As a joint time-frequency signal analysis tool, the wavelet transforms offer simultaneous interpretation of the signal in both time and frequency domains which results in signal filtering effects in both time and frequency dimensions. The detection process is carried out by input an electrical signal based on a single wavelet and the instantaneous output will undergo a wavelet transform to determine the ratio between the output and input wavelets.

Experimental results by the authors have shown significant improvement in accuracy when using the wavelets that the traditional FFT and the time averaging techniques.

The major objective of this paper is to demonstrate the success in using wavelet transform based noise reduction for accurate measurement of electrical signals due to material damages in CFRPs. The developed experimental system will conduct the studies of the relationships between the input electrical signals and simultaneously acquired of the electrical signal responses. The work conducted in this paper applies the time averaging, the FFT filtering, and both the continuous and discrete wavelet transform technologies in reducing the extraneous noises as well as enhancing the electrical signals for damage detection in CFRPs. Results are compared to indicate the accuracy as well as error involved in using the time averaging, FFT, and wavelet transform approaches with low and high noise levels of contaminations.

2. Signal Analysis Procedures

Signal analysis methods have been applied in material damage detection for many years (Doyle & Fernando, 1998; Whelan, 1999; Yan & Yam, 2002). The Fast Fourier Transform (FFT) is one of the most widely used signal analysis methods and is a perfect tool to extract the frequency information. Due to its signal averaging characteristics, when the signals have oscillating features in the time domain, the FFT procedure will not be capable to pinpoint the accurate occurring location and its amplitude. To overcome this drawback, there are currently a number of time-frequency methods, such as the short time Fourier transform (STFT), Wigner-Ville distribution (WVD) (Claasen et al., 1980), Choi-Williams distribution (CWD) (Choi & Williams, 1989) and both the discrete and the continuous wavelet transform (DWT & CWT) can be applied. Among these methods, CWT is the most favored because it has less cross-talk terms between the main frequencies as those observed in WVD and CWD. Also window of variable width can be employed in the CWT, which offers a more flexible way to observe simultaneously time and local spectral information than the STFT. Unlike Fourier analysis, which is often limited to sinusoid-based feature, wavelet methods have various wavelet functions. According to different morphological signals, a suitable wavelet function can be selected. The discrete wavelet transforms (DWT) adopt the digital filtering techniques to obtain the time-frequency representation and is widely used in signal compression and de-noising. In this section, the fundamental concept of wavelets will be presented followed by some comparisons of results from both continuous and discrete wavelet transforms.

Wavelet transforms basically have two distinct classes (Walker, 2008; Abbate et al., 2002): continuous wavelet transforms (CWT) and discrete wavelet transforms (DWT).

The definition of CWT is,

$$W(a,b) = \frac{1}{\sqrt{a}}\int_{-\infty}^{+\infty} x(t)\psi^*(\frac{t-b}{a})dt \tag{1}$$

Where ψ^*(t) is the complex conjugate of the analyzing wavelet function ψ(t) (mother wavelet), x(t) is a continuous time signal, *a* is the scaling parameter (corresponding to frequency), *b* is the shifting parameter (corresponding to time), and *W(a,b)* is a set of coefficients that is mapped by scaling parameter and shifting parameter. CWT is the sum over all time of the signal multiplied by scaled, shifted versions of the wavelet. The basic process starts with selection of the mother wavelet and compared to a section at the beginning of the original signal. The mother wavelet determines the characteristics of the resulting CWT in order to produce an effective wavelet transform, an appropriate mother wavelet has to be chosen. Generally speaking, the good choice of mother wavelet is the one with a similar shape to the original signal. The closer the similarity is, the more significant the coefficients obtained.

As to demonstrate the use of the wavelet transform, the CWT of a constant sine wave shown in Figure 1(a) and its resulting 3D time-frequency scalogram using the Mexican Hat wavelet is shown in Figure 1(b). The CWT scalogram shows a very even frequency component designated by the vertical axis and occurrence time by the horizontal axis as time progresses. Figure 2(a) shows the same sine wave with an additional pulse at the middle of the time period which leads to a spike from coefficients change at CWT time-frequency scalogram at the time location as shown in Figure 2(b). In order to demonstrate the proper selection of a mother wavelet based on morphological characterization, the signal with a mother wavelet in shape is calculated in the CWT using a similar shape wavelet function. A time function similar to the Morlet wavelet is created in Figure 3(a), and the CWT time-scaling scalogram using the Morlet wavelet is shown in Figure 3(b). The scalogram in Figure 3(b) illustrates that the high frequency occurs at the middle of period where the amplitude of the signal is presented by the color code while its frequency concentrations are shown by the vertical scaling parameter and the occurring times are shown by the horizontal axis. When a pulse is added to the wave function as shown in Figure

4(a), a downwards spike is produced at the low scaling/high frequency range showing the additional high frequency component adding to the original frequency components at the time of the pulse as shown in Figure 4(b). Based on these examples, one may conclude that the CWT scalogram can provide an accurate interpretation of the raw data at both time and frequency domains.

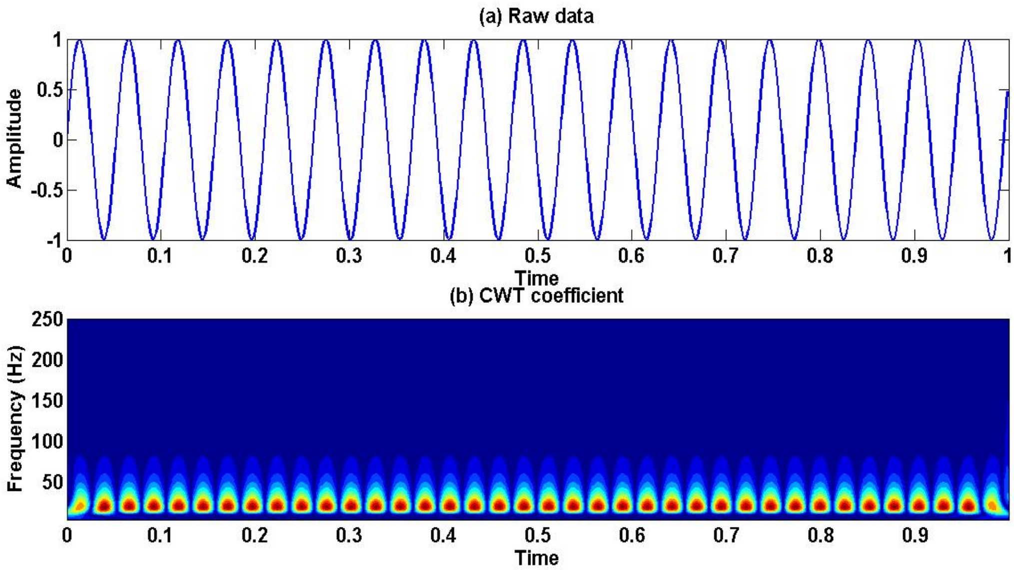

Figure 1. (a) Pure sine wave; (b) CWT time-frequency scalogram

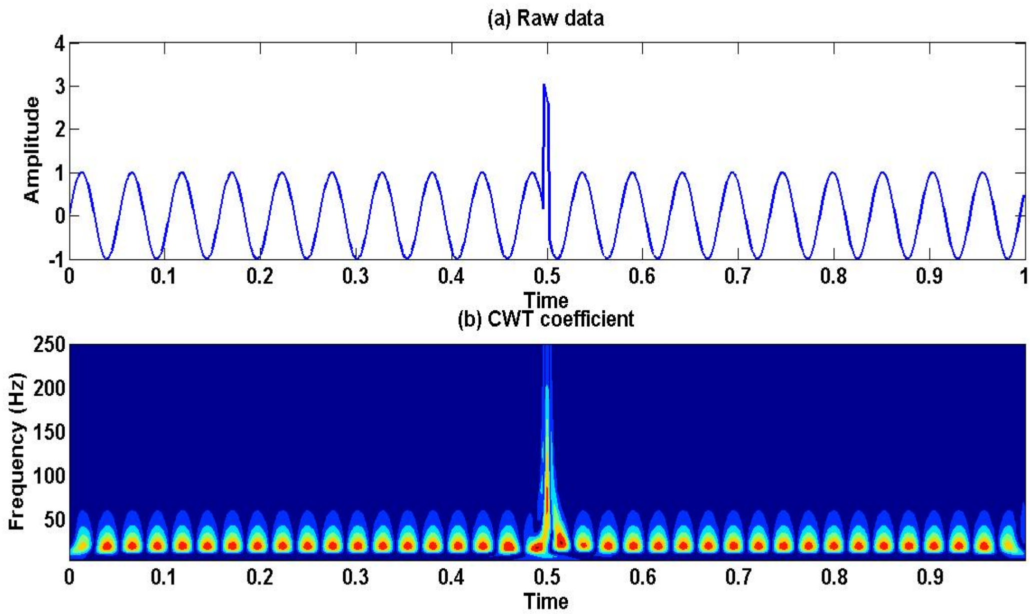

Figure 2. (a) Sine wave with a pulse; (b) CWT time-frequency scalogram

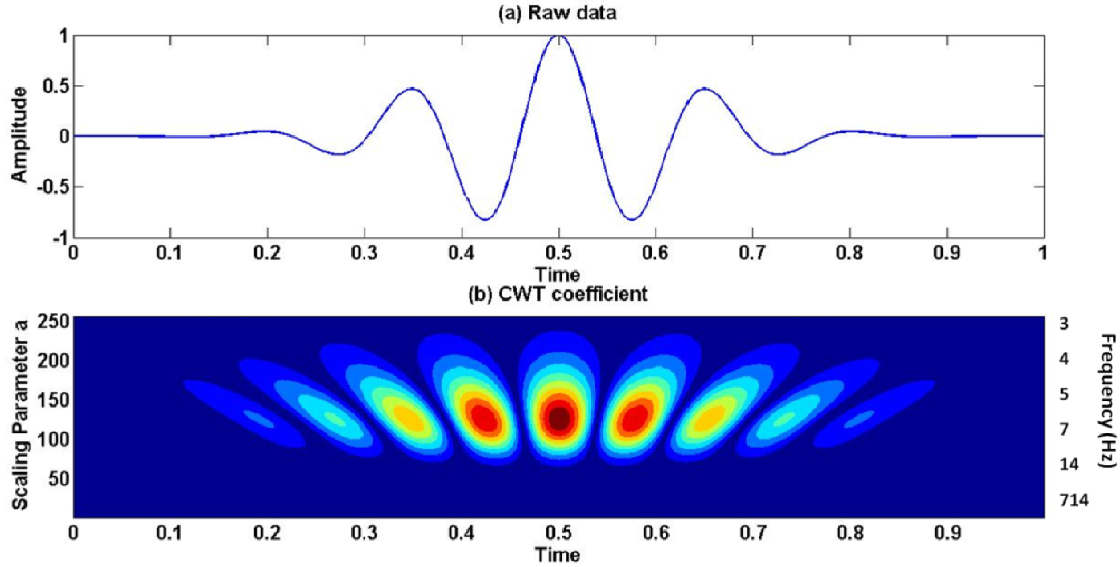

Figure 3. Morlet wavelet and CWT time-scaling scalogram

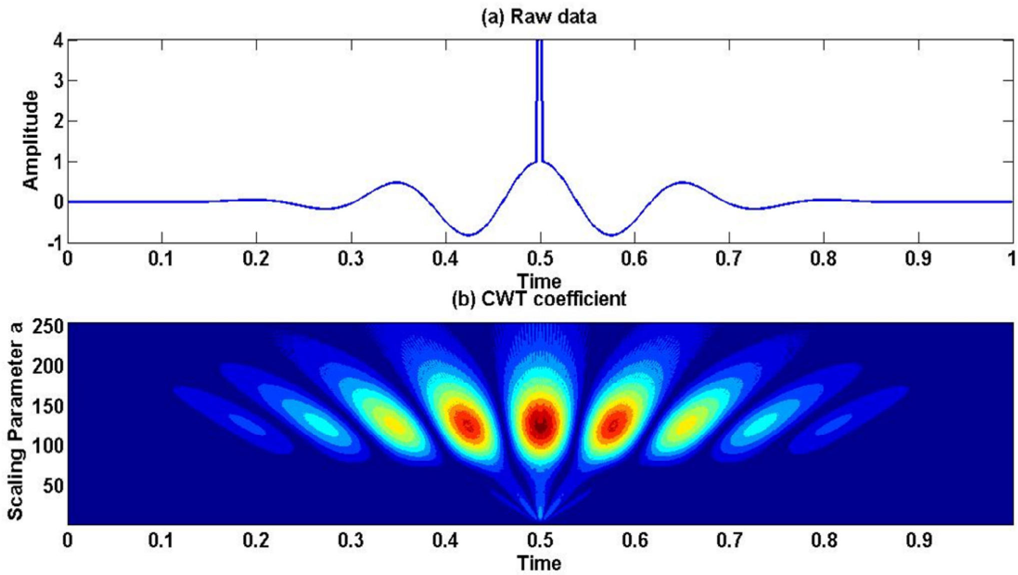

Figure 4. Morlet wavelet with a pulse and CWT time-scaling scalogram

The use of Discrete Wavelet Transform (DWT) has been traditionally used for de-noising by computing a series of high pass and low pass filtering of the signal. Then the decomposition at each level is represented by approximated and detailed coefficients until the signal is fully decomposed. The process can be demonstrated in a tree structure as shown in Figure 5. These coefficients can be reduced or set to zero to emphasize the particular feature of the signal and the threshold method is usually adopted in this step. A proper value is chosen as the threshold (T), and all detailed coefficients are set to zero if their absolute values are less than T. In the end, reconstruction of the coefficients will be achieved. Figure 6 shows a noisy sine function. The mother wavelet db5 is applied to this function with 5 levels of decomposition. S is the original signal, followed by a_5, the approximated coefficients, and d_5, d_4, …, d_1, the detailed coefficients at each level. After selecting a threshold of 0.85, the coefficients were constructed. Figure 7 illustrates as the black smooth curve is the de-noised signal after reconstruction, accompanied with the original signal. In this case of limited noise level, the DWT wavelet transform is found to be an effective tool to signal de-noising.

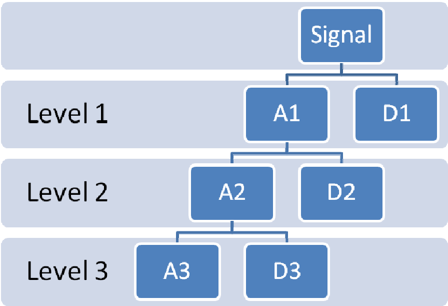

Figure 5. Discrete wavelet transform decomposition tree

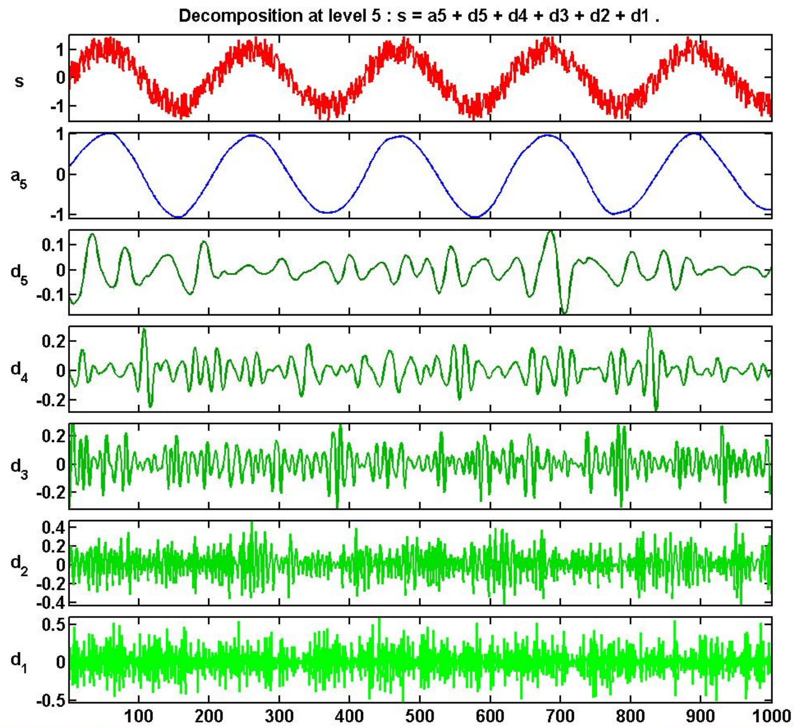

Figure 6. Noisy sine wave decomposition

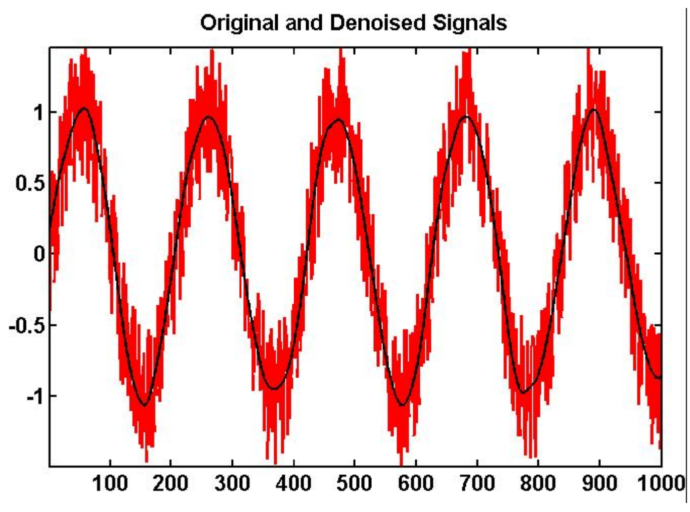

Figure 7. Denoised signal and original signal

3. Experimental Procedures

3.1 Self-sensing Electric Resistance and Potential Measurement

The electrical resistance measurement method has been widely employed for damage sensing and the four-probe method are commonly used in electrical resistance measurement for self-sensing in carbon fiber polymer-matrix composites. Although, the two-probe method shown in Figure 8(a) uses two electrical contacts which serve both current and voltage measurements is simpler but its sensitivity to the quality of the electrical contacts often makes it undesirable. In the four-probe method as shown in Figure 8(b), the outer two contacts are for the applied current while the inner twos are for voltage measurement. By using four contacts, the resistance of voltage contacts is not included in the resistance between the voltage contacts. Wang and Chung (Wang et al., 2006) have shown that the four-probe method is more sensitive and accurate than the conventional two-probe method in sensing impact damage in CFRPs. As an extension of the four-probe method, the multi-probe electric potential method as shown in Figure 8(c), has higher reliability for measurements of slight electric resistance changes in composite materials (Todoroki et al., 2003). In this work, the damage of the CFRP can be detected by measuring changes in the electric potential field on the surface. The current path is modified because of the fiber breakage and delamination, which results in changes around the damage zone (Angelidis & Iriving, 2007). In this method, two current electrodes and several voltage electrodes are attached on the surface of the specimen to adopt a four-probe method.

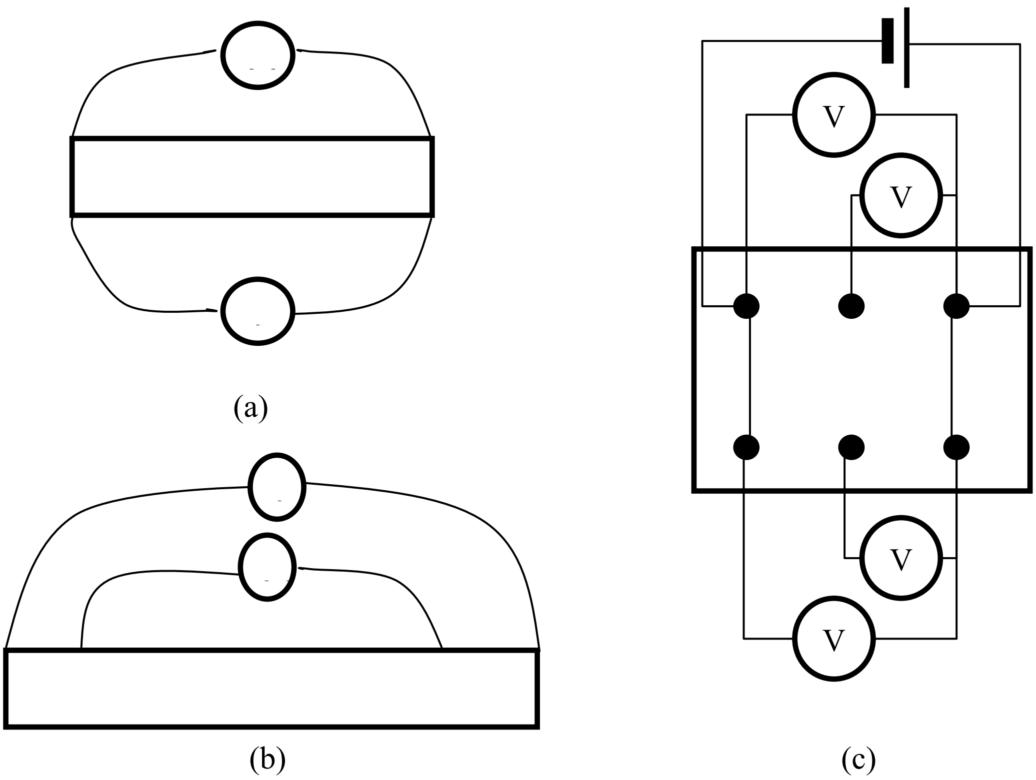

Figure 8. Electrical resistance measurement methods: (a) Two-probe method, (b) Four-probe method, and (c) Multi-probe method

3.2 Experimental Set-up

The wavelet transform has been applied for damage detection in CFRPs by using Lamb wave (Leavey et al., 2003; Yan et al., 2005) has been adopted for the electrical signal measurement in this research. The signal generation function provides the wavelet form signals, which results in more accurate analysis in further wavelet transform application. In this section, the experimental set-up and procedure are presented followed by the description of the test procedure.

3.2.1 Material Preparation

The specimen is carbon fiber reinforced epoxy polymer with a size of 2.83*2.83*0.02 in. Figure 9(a) shows the picture of the specimen. The surface of this CFRP sample was sanded first for the purpose of connecting carbon fibers with the electrodes well. Tiny holes were drilled at specific locations of the sheet to produce the appropriate electrodes. Silver Conductive Epoxy was deposited in all the holes with connecting wires as shown in Figure 9(b). This silver conductive epoxy is a mixer of pure silver epoxy adhesive, which provides a good combination of the adhesive properties of epoxy with the electrical properties of the silver. Even though the resistance of the silver conductive epoxy is low, it still has measurable influences on the resistances of the CFRP.

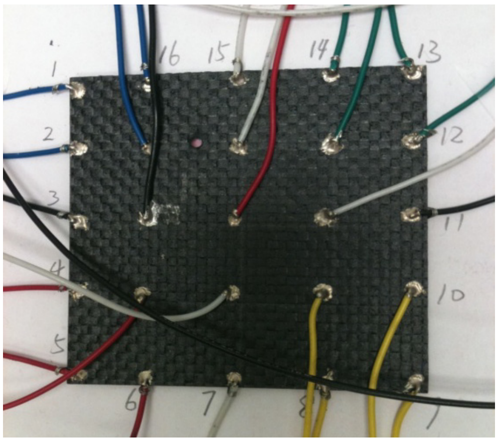

Figure 9. (a) CFRP sheet; (b) CFRP sheet with electrodes

There were 24 electrodes being used in this experiment. Eight of them were used for electrical generation, which connects to the Analog Output (AO) channels as red dots in Figure 10. The rest were connected to the Analog Input (AI) channels for the electrical signal acquisition, which are shown as blue dots in Figure 10. All the electrodes are named with numbers shown as the Figure 10 which is used throughout this work.

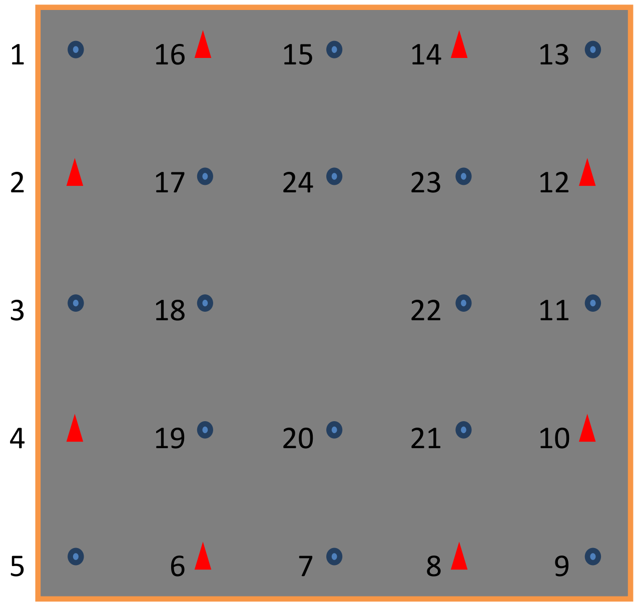

Figure 10. Scheme of CFRP sheet with electrodes

3.2.2 A/D and D/A Design

National Instrument DAQCard-6062E is used in this experiment. This DAQCard consists of 16 Analog Input channels with 12-bits resolution and 500 kS/s sample rate, and 2 Analog Output channels. The desktop connector NI SCB-68 was connected between the CFRP sheet and DAQ Card. The experimental set-up schematic is demonstrated in Figure 11. A National Instrument data acquisition system, which is accompanied with LabVIEW, assembles both Analog-to-Digital (A/D) and Digital-to-Analog (D/A) functions. Based on this application, the combined operating system including both A/D and D/A has been created to input a variety of input signal function, namely the constant DC, sinusoid, and wavelet waveform signals.

AO channels serve as D/A convertor for generating the electrical signals to the CFRP sheet through the 8 input locations marked in red dots in Figure 11. These 8 locations paired up into 2-12, 4-10, 6-16, and 8-14. For instance, 2-12 is chosen to be the input location, and the electrical signal is applied between 2 and 12. All 16 locations marked in blue dots are connected to AI single ended channels, and the electrical response signal is collected. Since either point 2 or point 12 is grounded, making a switch of these two input locations provides another set of response signals. The same procedure is repeated for the other pairs of input locations; they are 4-10, 6-16, and 8-14. There are 8 total sets of input combination. The purpose of multiple inputs is to locate the existing damage. The collected signals from 16 AI channels are varied because of different electrical input locations. The closer AI channels are to the input locations, the more sensitive response signals will be produced. Holes were introduced in the undamaged sheet in order to detect the damage.

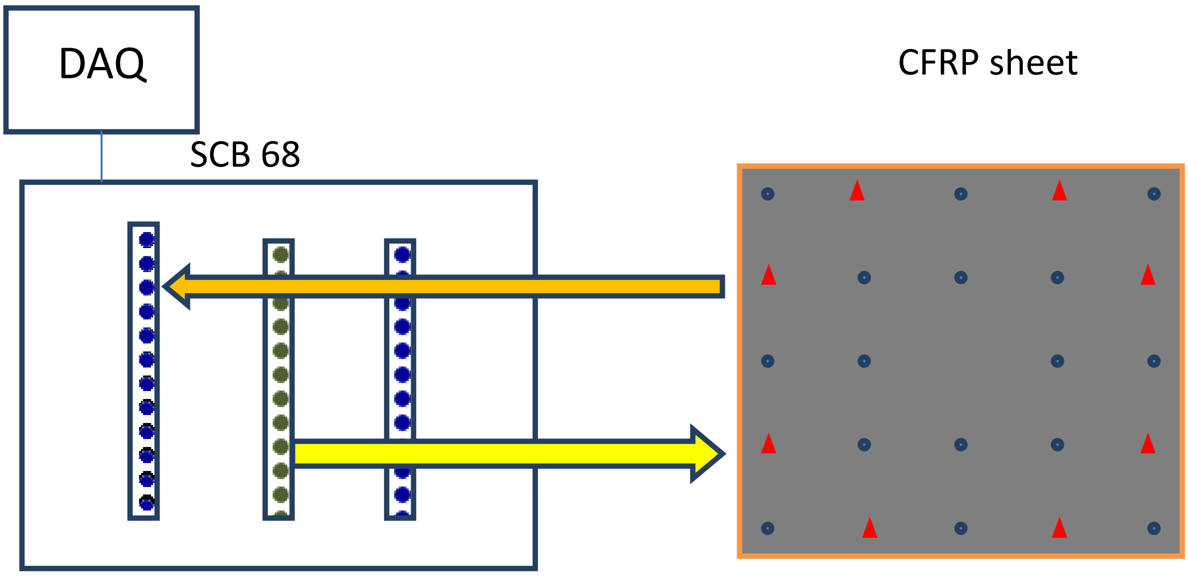

Figure 11. Experimental set-up schematic

4. Discussions of Results

4.1 Small Random Noise Effect

The noise with equal or smaller amplitude than the original signal is regarded as a small noise in this paper. For DC case, the original data used is a 0.03 V continuous signal. The random noise with the amplitude range of ±0.03 V is applied to influence the signal as shown in Figure 12(a). The noise effects can be reduced by averaging the data with an error to original signal of around 1%. However, since the random noise is unpredictable, the average of the signal can produce a large error. The same noise is used in the sine signal, too. The original sine signal is 200 Hz with 0.03 V of peak amplitude as shown in Figure 12(b). The frequency domain analysis is applied for noise filtering. First the FFT of the original signal at the top one of Figure 12(c) indicates the high amplitude at 200 Hz. When small amplitude of random noise, the FFT is able to filter out the noise and shows the significant amplitude at 200 Hz which is demonstrated in bottom plot of Figure 12(d). The error is 1.3% at 200 Hz.

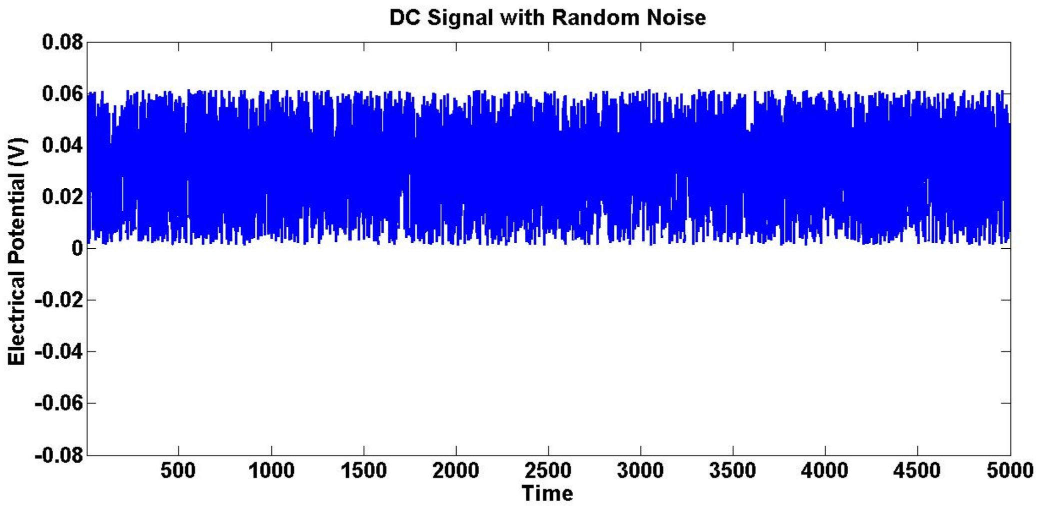

Figure 12(a). Small noise effect in DC signal

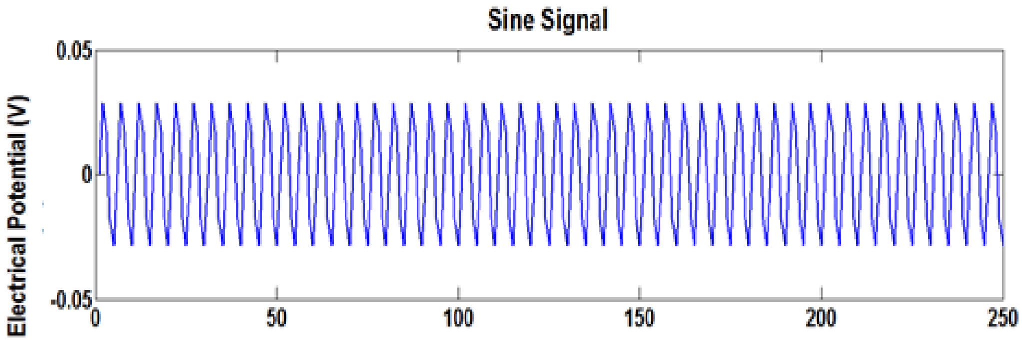

Figure 12(b). Original sine signal with no noise

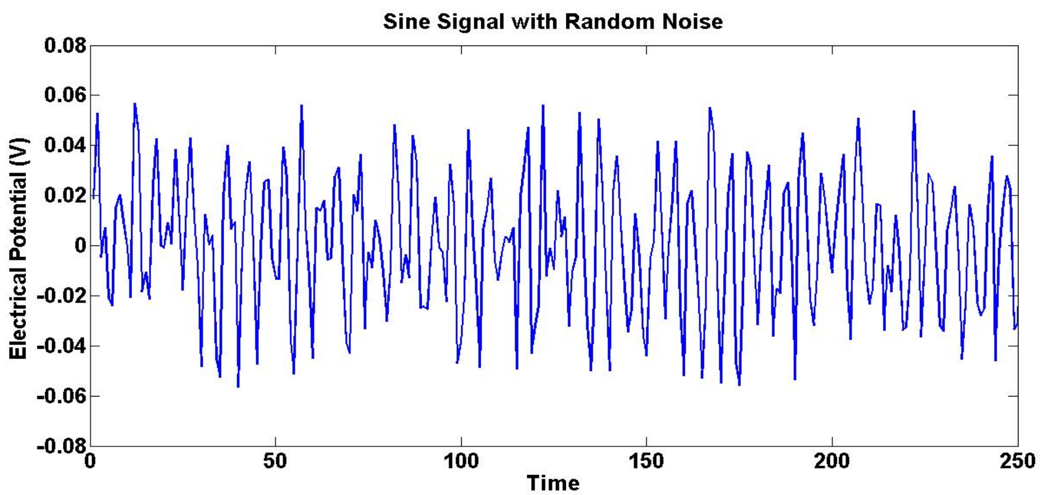

Figure 12(c). Sine signal with random noise

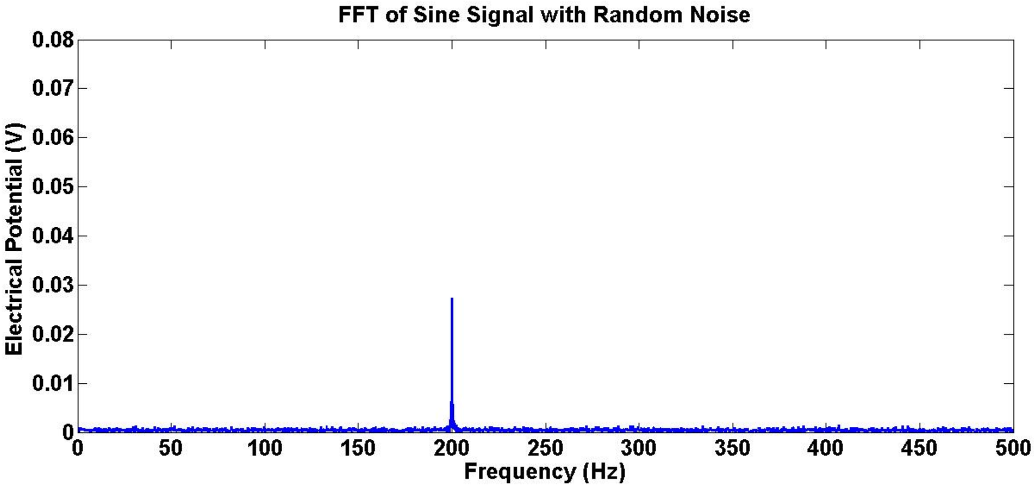

Figure 12(d). FFT of sine signal with random noise

In applying the CWT approach, the original wavelet signal of db10 in shape with maximum amplitude 0.03 V as shown in Figure 13(a) with the scalogram shown in Figure 13(b) with color scales of 1 to 500. The wavelet db10 is chosen for this transform, in order to obtain the high coefficients, high similarities, for the input time signal. The wavelet signal with small random noise and its wavelet coefficients are given in Figures 13(c) and (d).

The small random noises result in fluctuation, but the high coefficients still can be observed. As the region with high coefficients indicates the important information of the signal, 60% of the maximum coefficients were selected as the standard section to avoid the noise affected coefficients at the other sections. The wavelet coefficients are collected at the same standard section for the signal with noise. During this procedure, all values outside of the standard section have been filtered out, and only those significant coefficients are left. The scalograms are given in the Figures 14(a) and (b) for signals without and with random noise. These two scalograms present the percentage of the energy for each wavelet coefficient, which is also given the visualized denoising results. The error is found as 0.17%. It is hard to see the difference between these two scalograms since the random noise is too small to make tremendous influence. But this brings an idea that comparing the CWT coefficients is capable of observing the noise influence with few errors.

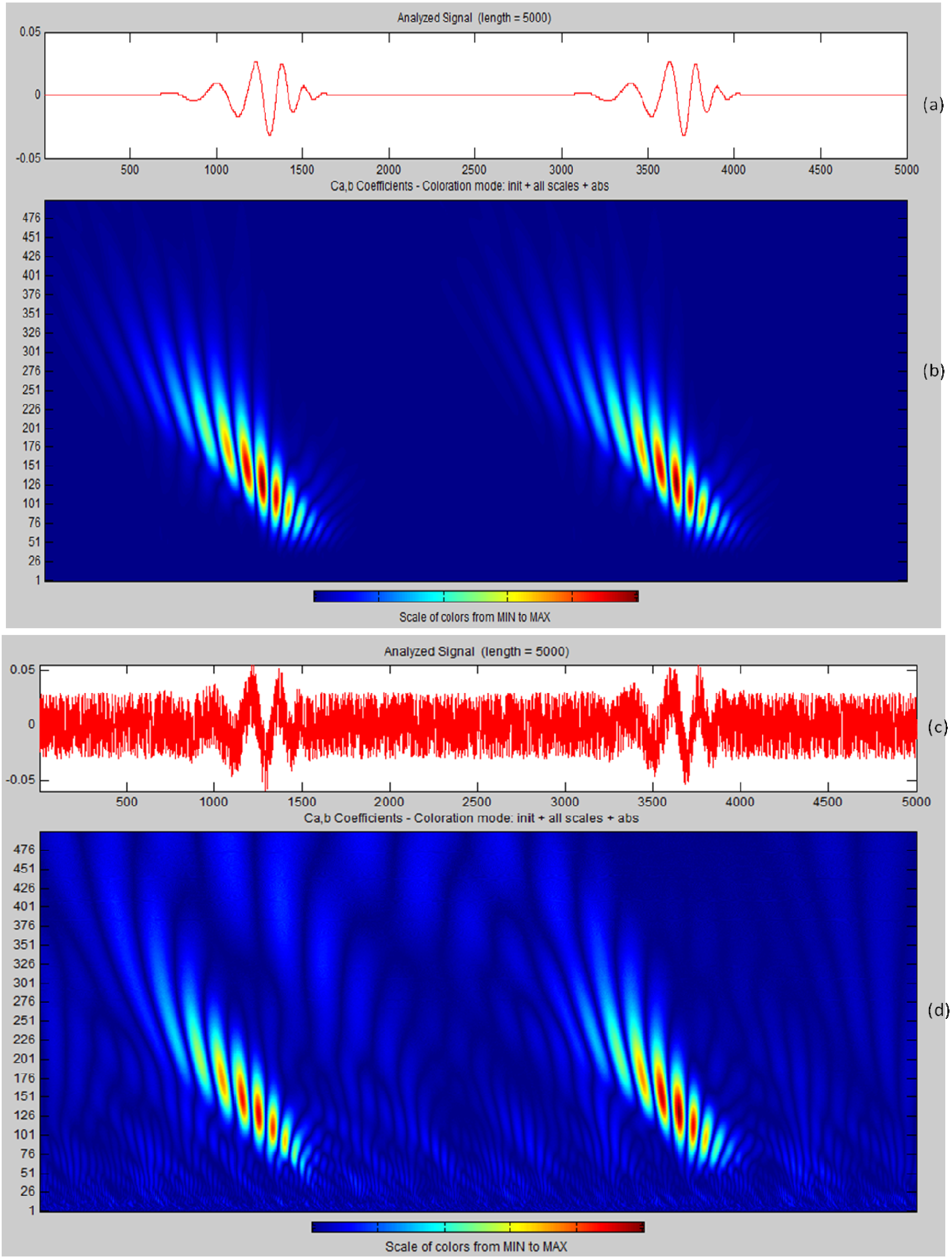

Figure 13. (a) and (b) wavelet signal without noise and its CWT coefficients; (c) and (d) wavelet signal with small random noise and its CWT coefficients

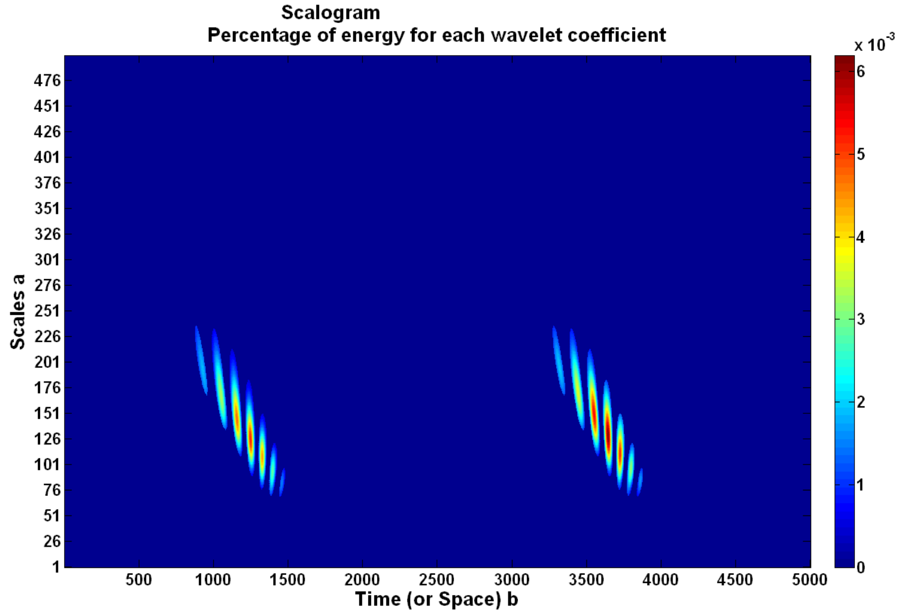

(a)

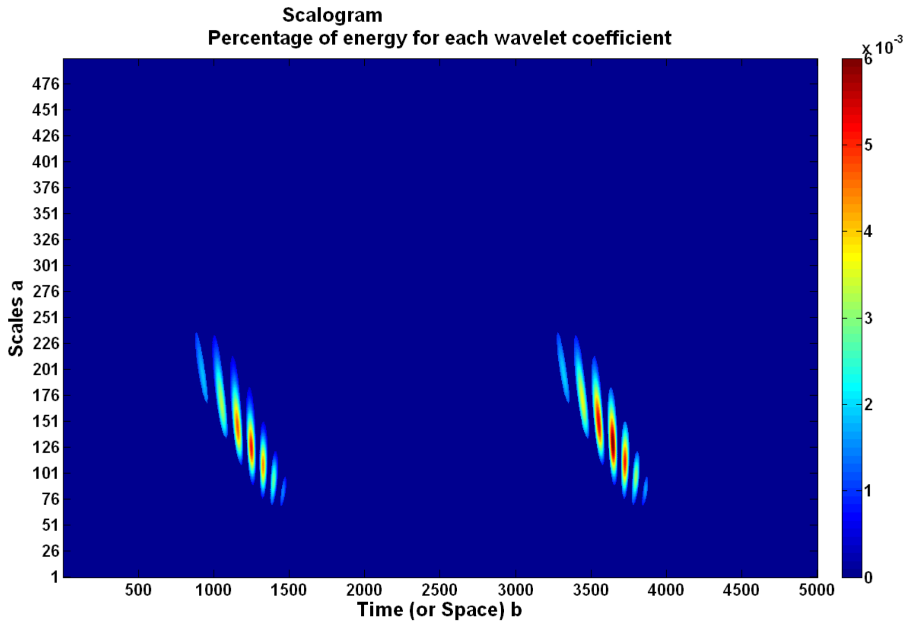

(b)

Figure 14. Scalogram of top 60% coefficients for wavelet signal (a) without noise; (b) with random noise

The other wavelet transform, DWT, offers the denoising technique of decomposing data into many levels and reconstructing the data. DWT by db10 is applied in this case. The denoised signal is obtained after 6 levels of decomposition and signal reconstruction. As shown in Figure 15, the signal with small random noise effect can be denoised and reverted to the similar shape to original signal.

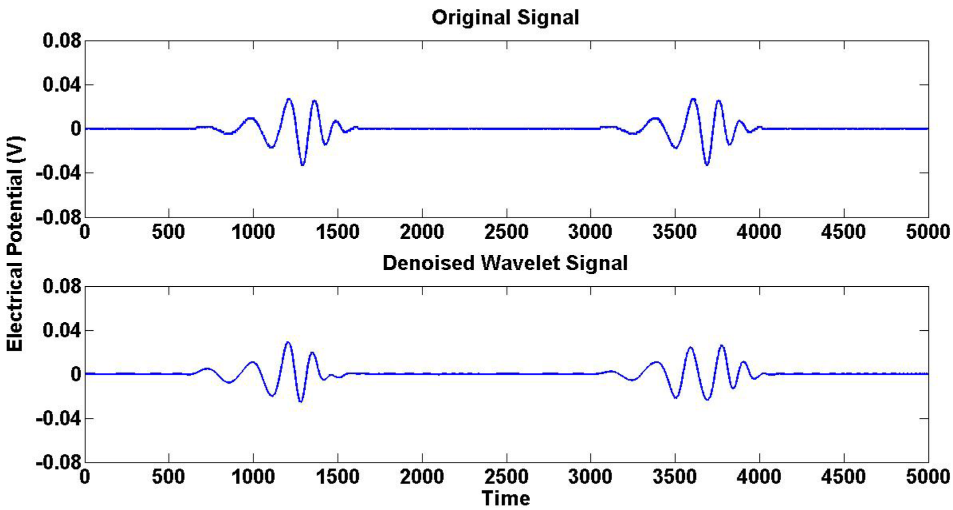

Figure 15. DWT of original signal and denoised signal with small random noise

4.2 Large Random Noise Effect

Figure 16(a) shows the DC signal with large random noise. The amplitude of original DC signal is 0.03 V, which stands for the data obtained from one channel. The range of random noise is within ±0.5 V. The signal becomes big fluctuated from the noise effect. By averaging the data, the error is found as 14%. It can be larger since the random noise effect is unpredictable.

The same noise is added to the sine signal. The original sine signal has 0.03 V in amplitude with 200 Hz in frequency. There are total 5000 samples. Figure 16(b) shows the part of the sine signal without and with the random noise. Frequency domain analysis method, FFT, is applied for filtering the noise in frequency domain. As shown in Figure 12(b), the significant peak occurs at the 200 Hz for the original sine signal. However, in the FFT of the signal with large random noise, there appears no remarkable high amplitude at 200 Hz. A comparison has been made to find the error ratio, 16%, at 200 Hz for both without and with noise signals. 0.03 V is obtained for data without noise while 0.035 V is for signal with noise. It is impossible to identify the frequency of original signal when the noise level is too high.

The same large random noise is applied to the wavelet form signal. Figure 17(a) indicates the huge influence of random noise to the original signal. It is really hard to tell the original shape of the signal. As the same procedure with small noise case, top 60% of CWT coefficients in magnitude at the standard section were selected and investigated. Comparing the coefficients in the standard section for both signals, the error is 1%, which is much less than the errors in the DC and FFT cases. The scalograms are presented in Figures 17 (b) and (c). The differences between two graphs in Figures 17 (b) and (c) can be observed because of the large random noise effect.

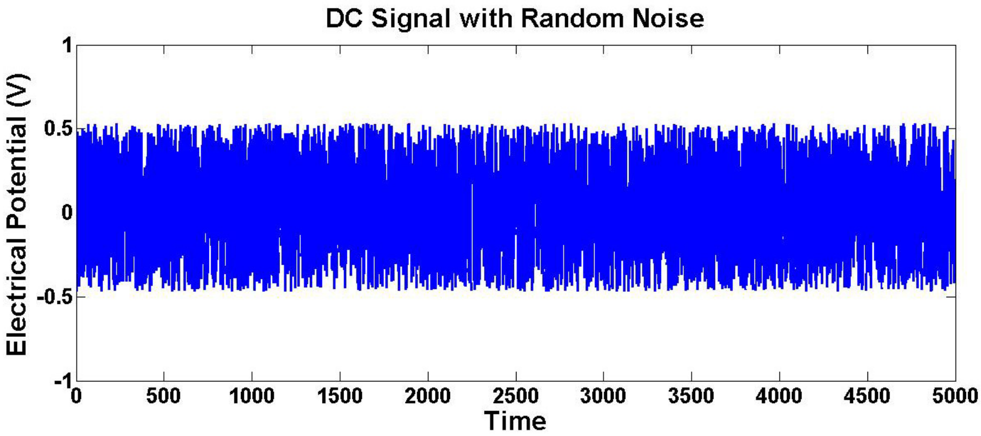

Figure 16(a). Large random noise effect at DC signal

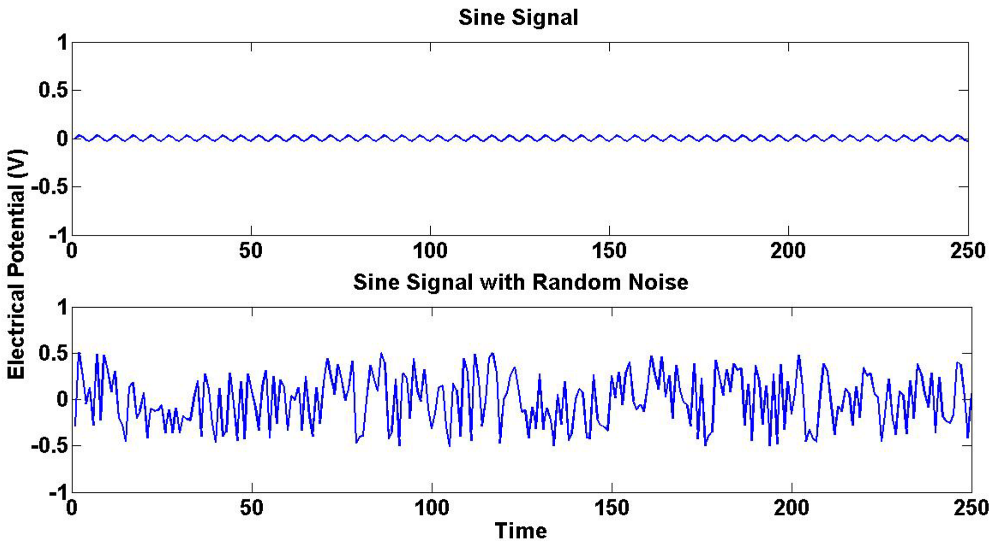

Figure 16(b). Partial sine signal without/with random noise

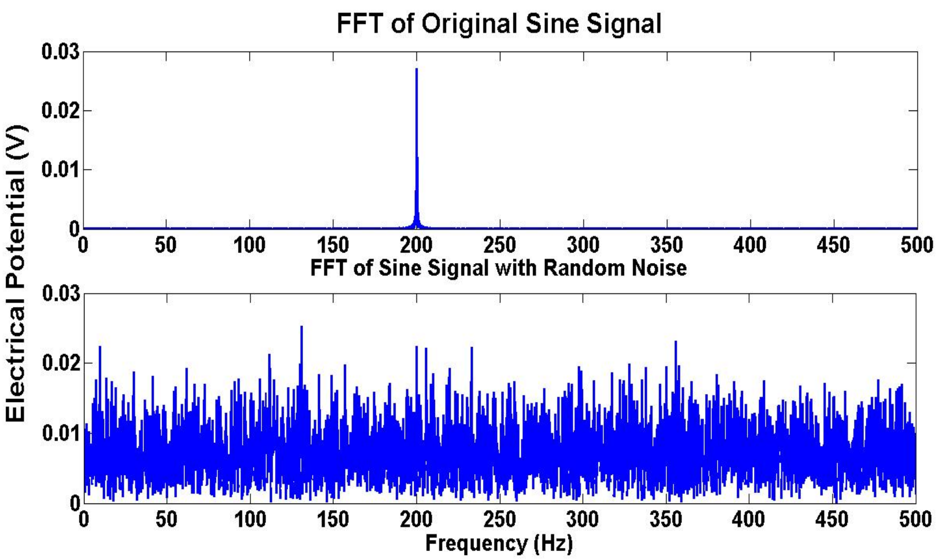

Figure 16(c). FFT of sine signal with large random noise effect

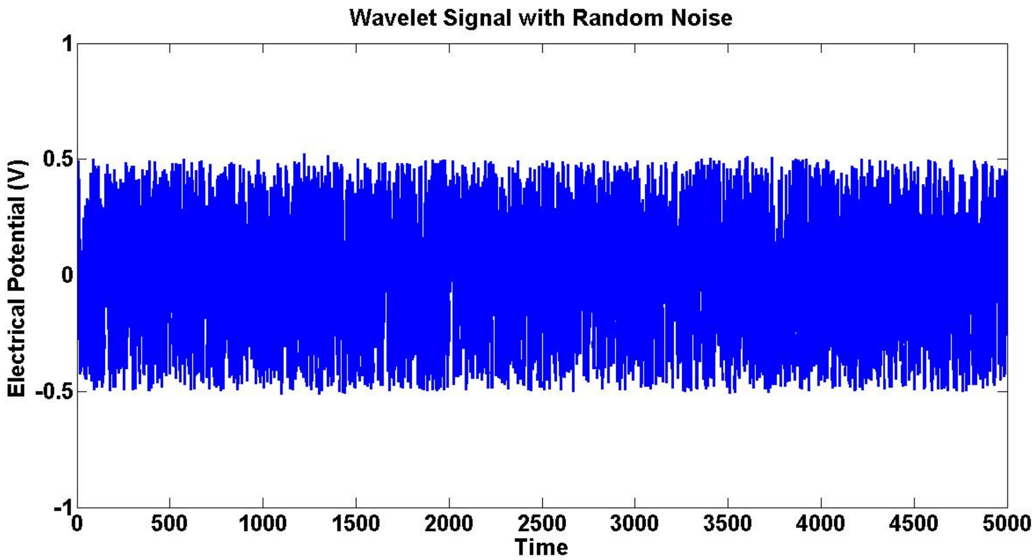

Figure 17(a). The wavelet signal with large random noise

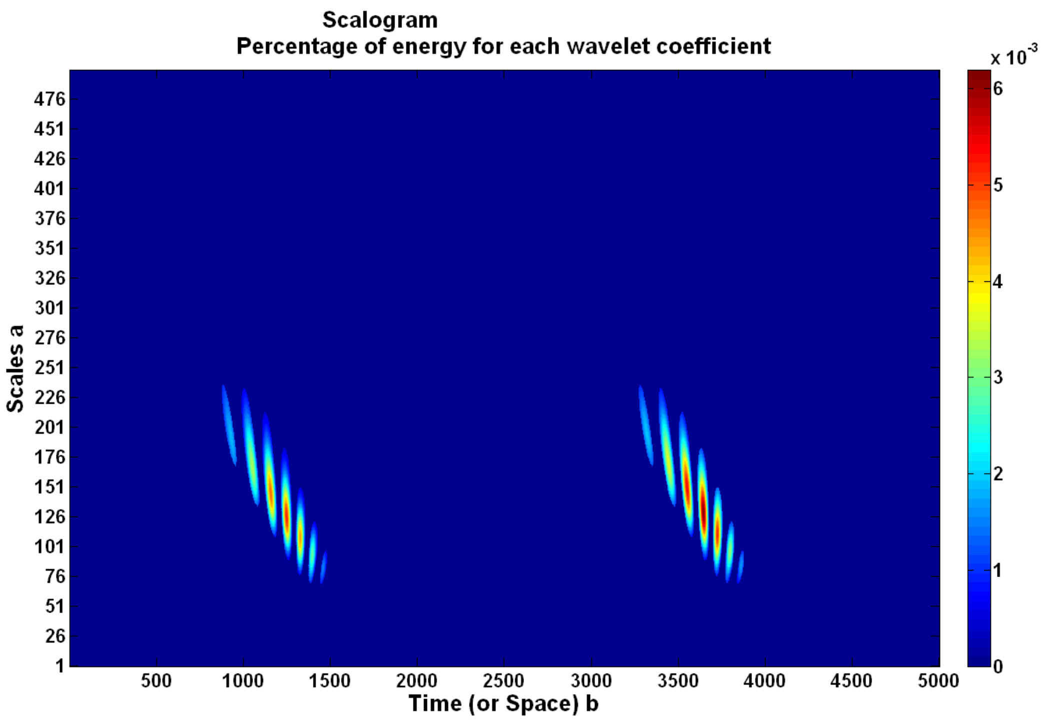

Figure 17(b). The scalogram for wavelet signal without noise

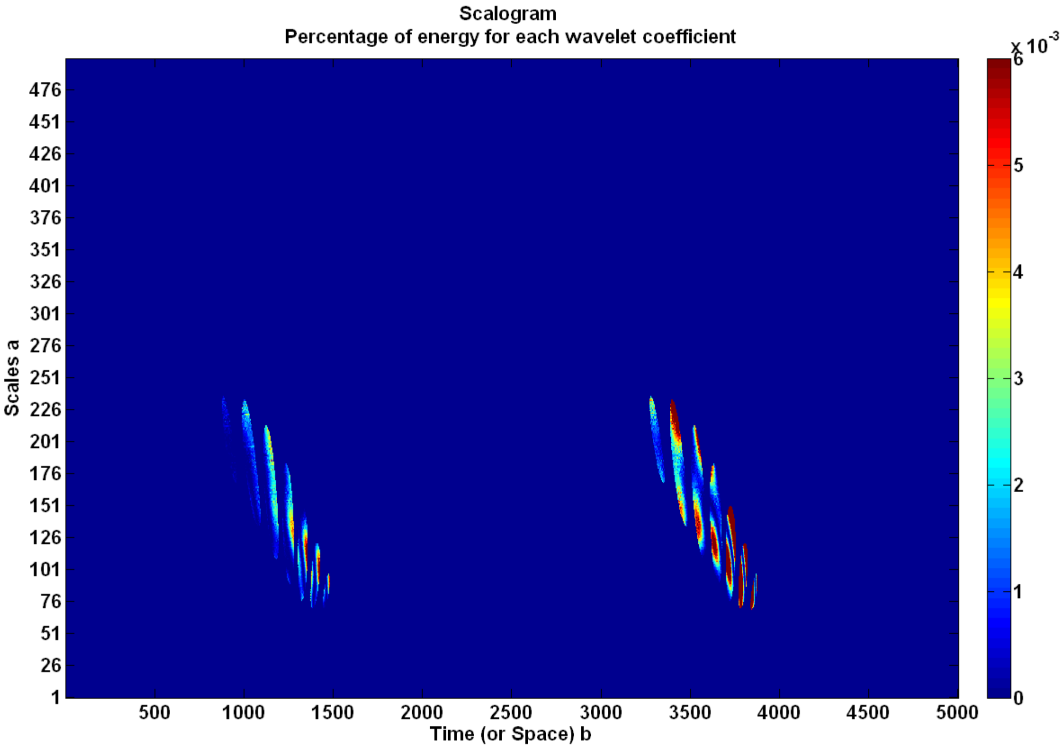

Figure 17(c). The scalogram for wavelet signal with noise

DWT is also conducted in the large random noise case. The wavelet db10 as original wavelet signal was selected for DWT. After 6 levels of decomposition, the signal was reconstructed as shown in the denoised signal of Figure 18. A substantial change in the wave form after denoising is found in the denoised signals after the DWT comparing to the original ones. Based on these results, one may conclude the DWT procedure may not be appropriate when high level noises are contaminated into the acquired signals.

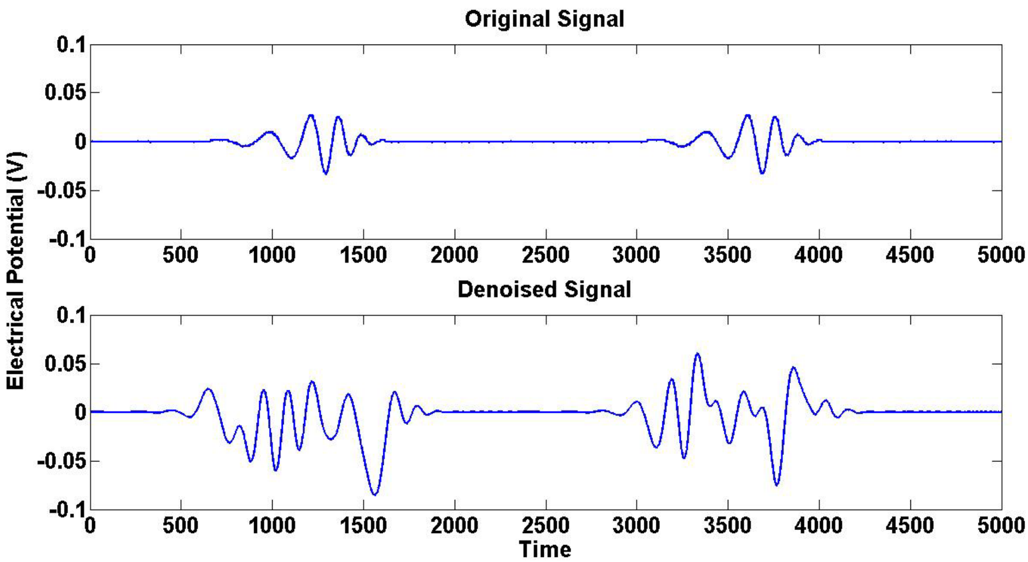

Figure 18. DWT of original signal and denoised signal with large random noise

For quantification purposes, Table 1 presents the comparisons of errors between the DC averaging, the FFT frequency filtering and the CWT procedures using the Signal-to-noise ratios (SNR) calculated and errors resulted from both small and large noise cases. Noted that, in Table 1, when low level of noises exist in the acquired signals, the use of CWT will reduce the errors from 1% at the averaging DC measurements to 0.17%. However, when a high level of noise contamination exists, the CWT will reduce the error of 14% from the averaging DC measurement to 1% using the CWT.

Table 1. SNR and error for DC, sine wave, and wavelet signals

	Small Noise		Large Noise	
	SNR	Error	SNR	Error
DC	3.29	1%	0.012	14%
Sine wave	1.61	1.3%	0.006	16%
Wavelet	121	0.17%	0.943	1%

In the CWT results presented for comparison in Table 1, the components above the top 60% of the wavelet coefficients with respect to the maximum wavelet amplitude is taken as the threshold standard for creating the joint time-frequency location selection criteria. A parametric study on the errors resulted using various top percentages as selection criteria are given in Table 2. One may note that the incurred errors can be significantly reduced by using the CWT time-frequency components over the 40% maximum amplitude than those over the 80% maximum amplitude. However, when a lower maximum amplitude criterion is selected, the number of data points will increase tremendously which will, in turn, will significantly increases the computational effort. During this study, the authors have found that a 60% of the maximum amplitude with less than one percent error, even for high noise level, is a good selection.

Table 2. Errors for different thresholds

	Errors				
Threshold	40%	50%	60%	70%	80%
Small Noise	0.005%	0.09%	0.17%	0.3%	0.7%
Large Noise	0.5%	0.8%	1%	2.6%	5.5%

5. Conclusions

This paper demonstrates the wavelet transform application in the noise reduction of the electrical measurement. When a small random noise affects the signal, both FFT and wavelet transforms can filter out the noise in either frequency or time-frequency domain. Even though, FFT and CWT are able to extract the correct signal when noise is small, the DWT is recommended since the signal can be reconstructed and can offer more information to compare to the original signal. The CWT is recommended when the random noise is large. Although it is not able to revert back to the original signal, the coefficient comparison offers valuable information to indicate the damage occurrences. When comparing the signal-to-noise ratios (SNR) for these three types of signals, it has been found that the CWT is far superior in reducing noise when the high level of noises are introduced into the acquired signals. In addition when high level of noises exist in the acquired signals, repeated uses of DWT will result in accumulated errors as shown in the results that the original shapes of the wavelet cannot be reconstructed. Further studies on using the CWT also shown that, when CWT components selected with lower amplitude ratio with the maximum component, significant increases in accuracy can be obtained. However, with the lower amplitude criteria, a much large number of points will be used and the computational effort will increase tremendously and may not be feasible in some cases.

References

Abbate, Agostino, de Cusatic, Casimer M., & Das, Pankaj K. (2002). *Wavelets and Subbands Fundamentals and Applications*. S.l.: Birkhauser Boston.

Angelidis, N., & Iriving, P. E. (2007). Detection of impact damage in CFRP laminates by means of electrical potential techniques. *Composite Science and Technology, 67*, 594-604.

http://dx.do.org/10.1016/j.compscitech.2006.07.033

Bai, W., & Wong, B. S. (2001). Evaluation of defects in composite plates under convective environments using lock-in thermography. *Measurement science and technology, 12*, 142-150.

Choi, H., & Williams, W. J. (1989). Improved time-frequency representation of multicomponent signals using exponential kernels. *IEEE Transactions on Acoustics, Speech, and Signal Processing, 37*(6), 862-871. http://dx.do.org/10.1109/ASSP.1989.28057

Claasen, T. A. C. M., & Mecklenbruker, W. F. G. (1980). The Wigner Distribution: a tool for time frequency signal analysis. *Philip Journal of Research, 35*, 372-389.

Doyle, C., & Fernando, G. (1998). Detecting impact damage in a composite material with an optical fiber vibration sensor system. *Smart Materials and Structures, 7*(4), 543-549.

Kaczmarek, H., & Maison, S. (1994). Comparative ultrasonic analysis of damage in CFRP under static indentation and low-velocity impact. *Composites science and technology, 51*, 11-26. http://dx.doi.org/10.1016/0266-3538(94)90152-X

Leavey, C. M., James, M. N., Summerscales, J., & Sutton, R. (2003). Damage detection in CFRP using wavelet scale correlation. *Materials Science Forum, 440-441*, 211-218.

Mook, G, Lange, R., & Koeser, O. (2001). Non-destructive characterisation of carbon-fibre-reinforced plastices by means of eddy-currents.*Composites science and technology, 61*, 865-873. http://dx.doi.org/10.1016/S0266-3538(00)00164-0,

Wang, X. J., & Chung, D. D. L. (1998). Short carbon fiber reinforced epoxy coating as a piezoresistive strain sensor for cement mortar. *Sensors and actuators A, 71*, 208-212.

Schulte, K., & Baron, C. (1989). Load and failure analyses of CFRP laminates by means of electrical resistivity measurements. *Composites science and technology, 36*, 63-76. http://dx.doi.org/10.1016/0266-3538(89)90016-X

Takeda, S, Obabe, Y., & Takeda, N. (2002). Delamination detection in CFRP laminates with embedded small-diameter fiber Bragg grating sensors. *Composites: Part A applied science and manufacturing, 33*, 971-980. http://dx.doi.org/10.1016/S1359-835X(02)00036-2

Todoroki, Akira, Tanaka, Miho, & Yoshinobu, Shimamura. (2004). Multi-prove electric potential change method for delamination monitoring of graphite/composite plates using normalized response surfaces. *Composites science and technology, 62*, 749-758. http://dx.doi.org/10.1016/j.compscitech.2003.08.004

Trappe, V., & Harbich, K. W. (2006). Intralaminar fatigue behaviour of carbon fibre reinforced plastics. *Internatioanl journal of fatigue, 28*, 1187-1196. http://dx.doi.org/10.1016/j.ijfatigue.2006.02.037

Walker, James S. (2008). *A Primer on Wavelets and Their Scientific Applications*.s. l.: Taylor & Francis Group, LLC.

Wang, S. K, Mei, Z., & Chung, D. D. L. (2001). Interlaminar damage in carbon fiber polymer-matrix composites, studied by electrical resistance measurement. *International journal of adhesion & adhesives, 21*, 465-471.

Wang, S. K., & Chung, D. D. L. (2002). Mechanical damage in carbon fiber polymer-matrix composite, studied by electrical resistance measurement. *Composite interfaces, 9*, 51-60. http://dx.doi.org/10.1016/10.1163/156855402753642890

Wang, S. K., Wang, D. J., & Chung, D. D. L. (2006). Method of sensing impact damage in carbon fiber polymer-matrix composite by electrical resistance measurement. *Journal of material science, 41*, 2281-2289. http://dx.doi.org/10.1007/s10853-006-7172-9

Whelan, M. (1999). Damage detection in vibrating composite panels using embedded fiber optic sensors and pulsed-DPSI. *Key Engineering Materials, 167-168*, 122-131.

Yan, Y. J., & Yam, L. H. (2002). Online detection of crack damage in composite plates using embedded piezoelectric actuators/sensors and wavelets analysis. *Computers and Structures, 58*(1), 29-38. http://dx.doi.org/10.1016/S0263-8223(02)00043-0

Yan, G., Zhou, L. L., & Yuan, F. G. (2005). Wavelet-based built-in damage detection and identification for composites. *Smart Structures and Materials 2005: Sensors and Smart Structures Technologies for Civil, Mechanical, and Aerospace Systems*, Proc. Of SPIE, Vol. 5765, pp. 324-334.